

February 2nd, 1996

MC-TH-96/06

## BOUND STATES OF TWO GLUINOS AT THE TEVATRON AND LHC

*E. Chikovani<sup>a</sup>, V. Kartvelishvili<sup>a,b</sup>,  
R. Shanidze<sup>a</sup> and G. Shaw<sup>b</sup>*

<sup>a</sup> High Energy Physics Institute, Tbilisi State University,  
Tbilisi, GE-380086, Republic of Georgia.

<sup>b</sup> Department of Physics and Astronomy, Schuster Laboratory,  
University of Manchester, Manchester M13 9PL, U.K.

### ABSTRACT

We calculate the production cross-sections for the vector and pseudoscalar bound states of two gluinos. It is shown that existing and future colliders imply a realistic chance of observing gluononium as a narrow peak in the two-jet invariant mass spectrum. With an integrated luminosity of  $0.2 \text{ fb}^{-1}$  at the Tevatron, and the high efficiency for tagging heavy quark jets at CDF, one should be able to detect vector gluononium for gluino masses up to about 170 GeV; or up to about 260 GeV for an upgraded Tevatron with a centre of mass energy of 2 TeV and an integrated luminosity of  $1 \text{ fb}^{-1}$ . The significantly higher energy and luminosity of LHC should allow pseudoscalar gluononium to be detected for gluino masses up to about 1500 GeV for an assumed luminosity of  $200 \text{ fb}^{-1}$ . These results are insensitive to the details of supersymmetry models, provided that R-parity is conserved and the gluinos are lighter than the squarks. In addition, gluononium detection implies a relatively accurate measure of the gluino mass, which is difficult to determine by other means.

# 1 Introduction

In most supersymmetry models [1], the ease with which gluinos can be detected depends critically on the relative masses of gluinos and squarks. If the gluino mass  $m_{\tilde{g}}$  is greater than the squark mass  $m_{\tilde{q}}$ , the gluino can decay to a squark and antiquark (or an antisquark and quark). This is a strong decay with a decay width of order  $\alpha_s m_{\tilde{g}}$ , which has prominent signatures, so that the Particle Data Group [2] give a current experimental lower limit of  $m_{\tilde{g}} \geq 218$  GeV. On the other hand, if the squarks are heavier than the gluino and R-parity is conserved, the gluino can only decay weakly, as shown in Figure 1, with a width of order [1]

$$\Gamma \approx \frac{\alpha \alpha_S m_{\tilde{g}}}{48\pi} \left( \frac{m_{\tilde{g}}}{m_{\tilde{q}}} \right)^4 \approx 5 \times 10^{-6} \left( \frac{m_{\tilde{g}}}{m_{\tilde{q}}} \right)^4 m_{\tilde{g}} . \quad (1)$$

The gluino is then more difficult to detect and the mass limit is reduced to 100 GeV [2]. However, in the latter case there is the possibility of observing the gluino indirectly, by detecting a gluino-gluino bound state. This has the advantage that the conclusions which can be drawn from a search for such states hold in a very wide class of supersymmetry models. In addition, the detection of such a state would lead to a relatively precise determination of the gluino mass, which could not be obtained easily by observing the decay products of the gluino itself, as some of these escape undetected. Here we investigate the possibility of detecting such states as narrow peaks in the di-jet invariant mass distributions, in the light of the significant improvements in heavy quark jet tagging and beam luminosity which have been achieved at the Tevatron, and in the light of the high energies and luminosities expected at the LHC.

# 2 Gluinonium

Gluinos are heavy spin-1/2 fermions which interact strongly via gluon exchange. Like gluons, they have no basic electroweak couplings. Hence, in contrast to top quarks, they live long enough to form two gluino bound states provided  $m_{\tilde{g}} < m_{\tilde{q}}$  as indicated above. The resulting spectrum of states is called gluinonium and has been studied in a number of papers [3]-[8]. For heavy gluinos, the low lying states are essentially Coulombic, with masses  $M \approx 2m_{\tilde{g}}$ , and they have much in common with heavy quarkonia. However, there are two important differences.

Firstly, the gluinos form a colour octet, so that there are six possible colour states for a two gluino system, corresponding to the well-known decomposition

$$8 \otimes 8 = 1 \oplus 8_S \oplus 8_A \oplus 10 \oplus \overline{10} \oplus 27 . \quad (2)$$

The single gluon exchange potential  $V(r)$  is attractive for the first three, and is related to the corresponding potential  $V_q(r)$  for  $q\bar{q}$  pairs by

$$V(r) = \left( \frac{9}{4}, \frac{9}{8}, \frac{9}{8} \right) V_q(r) \quad (3)$$

for the  $(1, 8_S, 8_A)$  states respectively.

Secondly, the gluino is a Majorana fermion with just two degrees of freedom. It is its own antiparticle and the Pauli principle applies to the two gluino system, thus forbidding certain states.

The resulting spectra of low lying states [3]-[5] are shown in Table 1. The allowed colour singlet 1 and symmetric octet  $8_S$  states have the same  $J^P$  values as the charmonium states with  $C = 1$ ; while the allowed antisymmetric colour octet  $8_A$  states have the same  $J^P$  values as the charmonium states with  $C = -1$ . In particular, the lowest lying colour singlet and symmetric colour octet states are the pseudoscalars  $\eta_g^0$  and  $\eta_g^8$  with  $J^P = 0^-$ , while the lowest lying antisymmetric colour octet state is vector gluonium  $\psi_g^8$  with  $J^P = 1^-$ .

The properties of these low lying states have been discussed previously [5]-[8]. Here we simply summarize the main results. All three  $L = 0$  states decay predominantly via gluino-gluino annihilation as shown in Figure 2. Specifically, the pseudoscalars  $\eta_g^{0,8}$  decay mainly to two gluons [3, 4, 5] with decay widths

$$\Gamma(\eta_g^0 \rightarrow g g) = \frac{18\alpha_S^2}{M^2} |R_0(0)|^2 \approx \frac{243}{8} \alpha_S^5 M \quad (4)$$

$$\Gamma(\eta_g^8 \rightarrow g g) = \frac{36\alpha_S^2}{M^2} |R_8(0)|^2 \approx \frac{243}{32} \alpha_S^5 M \quad (5)$$

while vector gluonium  $\psi_g^8$  decays predominantly into  $q\bar{q}$  pairs [7] with a decay width

$$\Gamma(\psi_g^8 \rightarrow q\bar{q}) = N_q \frac{2\alpha_S^2}{M^2} |R_8(0)|^2 \approx N_q \frac{27}{64} \alpha_S^5 M . \quad (6)$$

Here  $M \approx 2m_{\tilde{g}}$  is the gluonium mass,  $N_q$  is the number of quark flavours for which the decay is allowed kinematically, and quark masses have been neglected.  $R_{0,8}(0)$

are the radial wavefunctions of the corresponding two gluino systems evaluated at the origin. For simplicity, they have been approximated above by their values for a pure Coulombic potential, which is a good approximation for very heavy gluino masses. However, in our actual calculations we have also incorporated a linear confinement term [4], which increases the predicted widths by 40% (20%) for  $M=200$  GeV (600 GeV). Although much larger than the decay width (1) of the constituent gluinos, these decay widths are still very small compared to the gluononium mass  $M \approx 2m_{\tilde{g}}$ . The size of all three states is of order  $a^B \equiv 4(\alpha_s M)^{-1}$ , which is much smaller than the confinement length, thus justifying the relative stability of the colour octet states(see [1, 8]).

To summarise, vector gluononium  $\psi_{\tilde{g}}^8$  is a heavy compact object which behaves rather like a heavy gluon, except that its coupling to quarks is much stronger than its coupling to gluons. Hence it is most readily produced via  $q\bar{q}$  annihilation, and the Tevatron is at least a potentially promising place to look, being a source of both valence quarks and valence antiquarks. In contrast, the pseudoscalar states  $\eta_{\tilde{g}}^0$  and  $\eta_{\tilde{g}}^8$  couple predominantly to gluons, and can be produced equally well in both  $pp$  and  $\bar{p}p$  collisions via the gluon-gluon fusion mechanism. Their production cross-section increases more rapidly with energy than that for vector gluononium, and there is more chance of detecting them at the LHC. We discuss these possibilities in turn.

### 3 Vector Gluononium at the Tevatron

In this section we consider the possibility of observing vector gluononium as a peak in the di-jet invariant mass distribution at the Tevatron. This possibility has been enormously enhanced since the previous study [7], by improvements in the efficiency of heavy quark jet tagging at CDF [9] and by the increase of the Tevatron luminosity.

The vector gluononium is produced and decays in  $p\bar{p}$  collisions via the subprocess

$$q + \bar{q} \rightarrow \psi_{\tilde{g}}^8 \rightarrow q + \bar{q}, Q + \bar{Q} \quad (7)$$

where we use the symbols  $q = u, d, s$  and  $Q = c, b, t$  to distinguish light and heavy quarks<sup>1</sup>.

---

<sup>1</sup>Obviously,  $t$ -quarks contribute only if the gluino is heavy enough, and even then for the range of gluino masses accessible at the Tevatron this contribution is strongly suppressed by the available phase space. So, in our rough estimates we consider just two "taggable" heavy quark flavours, though in the full simulation correct mass-dependent branching fractions have been used.

The nature of the background depends on the value of the ratio  $M/\sqrt{s}$ . At Tevatron energies, the range of interest lies mainly in large values  $M/\sqrt{s} > 0.2$ , where the luminosity of colliding  $q\bar{q}$  pairs prevails over the gluon-gluon pairs. In this region, the main sources of two-jet background are the subprocesses

$$q + \bar{q} \xrightarrow{QCD} g + g, \quad q + \bar{q}, \quad Q + \bar{Q} \quad (8)$$

where the first two have the angular dependence

$$\frac{d\sigma}{d \cos \theta^*} \propto (1 - \cos^2 \theta^*)^{-2}.$$

That is, they peak sharply at  $\cos \theta^* = \pm 1$ , where  $\theta^*$  denotes the scattering angle in the centre of mass frame of the two jets. In contrast, the signal from the subprocess (7) has a much weaker dependence

$$\frac{d\sigma}{d \cos \theta^*} \sim 1 + \cos^2 \theta^*.$$

Hence, a cut  $|\cos \theta^*| < z$  should improve the signal-to-background ratio. However, if the cut  $z$  is too low, the signal detection efficiency is low. The optimum value of  $z$  in this case is close to 2/3.

The usefulness of heavy quark tagging is clearly brought out by considering the production ratios for the various final states in both the signal (7) and background (8). The relative contribution of the three background subprocesses in (8) at small  $|\cos \theta^*|$  is given by [7, 10]

$$gg : q\bar{q} : Q\bar{Q} = 14 : 65 : 6, \quad (9)$$

while for the signal (7) one has

$$gg : q\bar{q} : Q\bar{Q} = 0 : 3 : 2. \quad (10)$$

Hence by tagging the heavy quark jets one reduces the background by a factor of  $85/6 \approx 14$ , while retaining 40% of the signal. At larger  $|\cos \theta^*|$  the gain in the signal-to-background ratio caused by heavy quark jet tagging will be even larger.

At smaller gluionium masses  $M \approx 2m_{\tilde{g}} < 200$  GeV, initial gluons contribute much more significantly to the background, even with heavy quark jet tagging, through the subprocess

$$g + g \xrightarrow{QCD} Q + \bar{Q}. \quad (11)$$

This makes the signal-to-background ratio hopelessly small for any reasonable jet-jet invariant mass resolution. However, this region of gluino masses is already covered by other methods.

So, most of the two-jet QCD background at large invariant masses arises from light quark and gluon jets, and the signal-to-background ratio can be significantly enhanced by triggering on heavy quark jets [7]. To check that this makes the detection of vector gluinonium a viable possibility at the Tevatron, we have simulated both the gluinonium signal and the 2-jet QCD background using the PYTHIA 5.7 Monte Carlo event generator [11]. The vector gluinonium production and decay was simulated by exploiting the fact that  $\psi_{\tilde{g}}^8$  behaves much like a heavy  $Z'$  with axial current and lepton couplings set to zero and a known mass-dependent vector current coupling to quarks, chosen to comply with the corresponding decay width after taking into account appropriate colour and flavour counting. This effective coupling included the non-Coulomb corrections mentioned earlier, and an enhancement due to the fact that numerous radial excitations of the  $\psi_{\tilde{g}}^8$ , which could not be separated from it for any reasonable mass resolution, will also contribute. These yield an overall factor of between 1.8 and 1.6 depending on  $M$ , and the resulting effective vector coupling  $a_V$  falls exponentially from  $a_V = 0.225$  at  $M = 2m_{\tilde{g}} = 225$  GeV to  $a_V = 0.172$  at  $M = 2m_{\tilde{g}} = 450$  GeV. This signal sits on a much larger background, which has been simulated on the assumption that it arises entirely from the leading order QCD subprocesses for heavy quark pair production (8) and (11). A constant  $K$  factor  $K = 2.0$  has been used for both signal and background.

The cross section for vector gluinonium production at the Tevatron is shown in Fig. 3 for  $\sqrt{s} = 1.8$  TeV. Only decays into heavy quark-antiquark pairs were taken into account, and a heavy quark jet tagging efficiency of 50% was assumed. The cut on the jet angle  $\theta^*$  in the two-jet c.m.s. frame is  $|\cos \theta^*| < 2/3$ , and the cut on jet rapidity  $y$  is  $|y| < 2.0$ . The analysis shows that with an integrated luminosity of 200 pb<sup>-1</sup> one can hope to see the gluinonium signal from gluinos with masses up to 140 GeV as a 5 standard deviation peak, and the signal from gluinos with masses up to 170 GeV as a 3 standard deviations peak. The signal-to-background ratio is around 7 – 10% at the peak for the assumed two-jet invariant mass resolutions of 25 GeV, 30 GeV and 38 GeV at  $M = 225$  GeV, 320 GeV and 450 GeV respectively [9, 12].

For an upgraded Tevatron with the energy increased to 2.0 TeV and an integrated

luminosity of  $1000 \text{ pb}^{-1}$ , the reach is significantly higher. The cross-section obtained with the same cuts and the same assumptions about the detector resolution and heavy quark jet tagging efficiency is shown in Fig. 4. In this case one can hope to see the gluinonium signal from gluinos with masses up to 220 GeV as a 5 standard deviation peak, and the signal from gluinos with masses up to 260 GeV as a 3 standard deviation peak. Finally, we note that the statistical significance of the peak is essentially inversely proportional to the two-jet invariant mass resolution, so the reach can be significantly extended if some way is found to improve the latter.

## 4 Pseudoscalar Gluinonium at the LHC

Pseudoscalar gluinonium can also be detected as a peak in the di-jet invariant mass distribution. However, both  $\eta_g^0$  and  $\eta_g^8$  decay predominantly into gluon jets, which are also the main component of the background. Quark jet tagging does not help in this case, and one must rely on high statistics and good resolution to separate the signal from the background. These can hopefully be achieved at LHC, as we shall now discuss.

Pseudoscalar gluinonium is produced, as we have noted, via the subprocess

$$g + g \rightarrow \eta_g^{0,8} \rightarrow g + g \quad (12)$$

while the 2-jet background in  $pp$  collisions is dominated by the gluon scattering QCD subprocess

$$g + g \xrightarrow{QCD} g + g \quad (13)$$

with some contribution from the valence light quark elastic scattering subprocesses

$$g + q \xrightarrow{QCD} g + q, \quad q + q \xrightarrow{QCD} q + q \quad (14)$$

at higher values of  $M/\sqrt{s}$ . Once again, the angular dependence of the background has large peaks in the forward and backward directions,  $d\sigma/d\cos\theta^* \propto (1-\cos^2\theta^*)^{-2}$ , while the signal is isotropic in the two jet centre of mass frame. Thus a cut  $|\cos\theta^*| < z$  with optimal  $z$  close to 0.6 will increase the signal-to-background ratio.

To check that pseudoscalar gluinonium detection is a viable possibility at the LHC, we have again simulated the QCD background, including all the above subprocesses, using the PYTHIA 5.7 generator [11]. Gluinonium production has not

been explicitly implemented in PYTHIA, but all we need is a pseudoscalar object of the right mass which is produced by gluon gluon fusion and decays to two gluons. In other words, pseudoscalar gluonium behaves like a pseudoscalar state of heavy quarkonia with appropriately adjusted mass, couplings and width. In this way the signal can also be simulated in PYTHIA, where we have again used a K-factor of 2.0 and an enhancement factor of 1.5 to allow for the fact that numerous radial excitations of the  $\eta_g^0$  and  $\eta_g^8$ , which could not be separated from them for any reasonable mass resolution, will also contribute. In addition one can not separate the signals from  $\eta_g^0$  and  $\eta_g^8$  either, so a single effective width  $\Gamma$  has been used to describe the production of all pseudoscalar gluonium states. This effective width was calculated by summing properly weighted widths (4) and (5), with non-Coulomb corrections and higher resonance contributions included, giving  $\Gamma = 0.85 \text{ GeV}$ ,  $1.1 \text{ GeV}$  and  $1.6 \text{ GeV}$  for  $M = 200 \text{ GeV}$ ,  $600 \text{ GeV}$  and  $2 \text{ TeV}$ , respectively.

The resulting cross section for pseudoscalar gluonium production at the LHC is shown in Fig. 5. The cut on the jet angle  $\theta^*$  in the two-jet centre of mass frame is  $|\cos \theta^*| < 2/3$ , and the cut on jet rapidity  $y$  is  $|y| < 2.5$ . The estimated two-jet invariant mass resolution varies from  $22 \text{ GeV}$  at  $M = 300 \text{ GeV}$  to  $32 \text{ GeV}$  at  $M = 600 \text{ GeV}$  and  $50 \text{ GeV}$  at  $M = 2 \text{ TeV}$  [13]. The signal-to-background ratio is smaller than in the previous section, of order 1-2%, but the much higher luminosity of LHC leads none the less to a higher reach in gluino mass. As can be seen in Fig. 5, with a luminosity of  $10^4 \text{ pb}^{-1}$  one expects to reach the gluino masses  $800$  ( $1000$ )  $\text{GeV}$  at  $5$  ( $3$ ) standard deviations, while for the highest likely integrated luminosity of  $2 \cdot 10^5 \text{ pb}^{-1}$  gluino masses up to  $1300$  ( $1500$ )  $\text{GeV}$  could be covered.

## 5 Conclusions

We have studied the production characteristics of various bound states of two gluinos (gluonium) for existing and future hadronic colliders. We conclude that gluonium states can be detected as narrow peaks in the di-jet invariant mass spectra, effectively complementing more traditional gluino searches, in the case when the gluino is lighter than the squarks.

In  $p\bar{p}$  collisions one expects copious production of vector gluonium, which decays predominantly to  $q\bar{q}$  pairs. The high efficiency of the heavy quark jet tagging

at CDF, together with the boost of the Tevatron luminosity, should allow one to reach gluino masses of 140-170 GeV at  $\sqrt{s} = 1.8$  TeV, and  $200 \text{ pb}^{-1}$  and 220-260 GeV at  $\sqrt{s} = 2.0$  TeV and  $1000 \text{ pb}^{-1}$ , with realistic efficiencies, resolutions and experimental cuts taken into account.

In  $pp$  collisions pseudoscalar gluinonium production is quite large, again allowing one to look for a narrow peak in di-jet invariant mass spectra in spite of the high background from QCD scattering subprocesses. The high luminosity of the LHC, together with the high design resolutions of the ATLAS and CMS detectors, should allow one to reach gluino masses of  $800 - 1000$  GeV at  $\sqrt{s} = 14$  TeV and  $10^4 \text{ pb}^{-1}$ , while for the highest likely integrated luminosity  $2 \cdot 10^5 \text{ pb}^{-1}$  the reach increases to  $1300 - 1500$  GeV.

Finally, we note that if gluinonium is observed, its mass can be determined with an accuracy of a few GeV. This makes gluinonium detection by far the most precise way of measuring the gluino mass, since the binding energy inside gluinonium is very small and calculable.

## References

- [1] H.R. Haber and G.L.Kane *Phys. Rep.* **117**, 75 (1984).
- [2] Review of Particle Properties, *Phys. Rev. D* **50**, 1173 (1994).
- [3] W.Y. Keung and A. Khare, *Phys. Rev. D* **29**, 2657 (1984).
- [4] J.H. Kühn and S. Ono, *Phys. Lett. B* **142**, 436 (1984).
- [5] T. Goldman and H.E. Haber *Physica* **15D**, 181 (1985).
- [6] A. Hoch and V.G. Kartvelishvili, *Phys. Lett. B* **201**, 546 (1988).
- [7] E.G. Chikovani, V.G. Kartvelishvili and A.V. Tkabladze, *Z. Phys. C* **43**, 509 (1989).
- [8] E.G. Chikovani, V.G. Kartvelishvili and A.V. Tkabladze, *Sov. J. Nucl. Phys.* **51**, 546 (1990).
- [9] J. M. Benlloch, Talk given at XXXth Rencontres de Moriond, Les Arcs, March 1995.
- [10] E. Eichten et. al. *Rev. Mod. Phys* **56**, 579 (1984).
- [11] T. Sjöstrand, “PYTHIA 5.7 and JETSET 7.4, Physics and Manual,” CERN report TH-7112/93
- [12] F. Abe et al. (CDF Collaboration), *Phys. Rev. D* **41**, 1722 (1990).
- [13] For a fuller discussion see E.G. Chikovani, V.G. Kartvelishvili and R. Shanidze, CMS Technical note TN/93-125, CERN, Geneva 1993; and *Proc. of the Georgian Physical Society* **A2**, 132 (1994).

1	$8_S$	$8_A$
$^1S_0$	$0^- (\eta_{\tilde{g}}^0)$	$0^- (\eta_{\tilde{g}}^8)$
$^3S_1$		$1^- (\psi_{\tilde{g}}^8)$
$^1P_1$		$1^+$
$^3P_0$	$0^+$	$0^+$
$^3P_1$	$1^+$	$1^+$
$^3P_2$	$2^+$	$2^+$
$^1D_2$		$2^-$
$^3D_1$	$1^-$	$1^-$
$^3D_2$	$2^-$	$2^-$
$^3D_3$	$3^-$	$3^-$

**Table 1.** Spin-parities  $J^P$  for the low lying states of gluinonium with  $L \leq 2$ . The three columns correspond to the colour singlet state 1 and the symmetric and antisymmetric colour octet states  $8_S$  and  $8_A$  respectively.

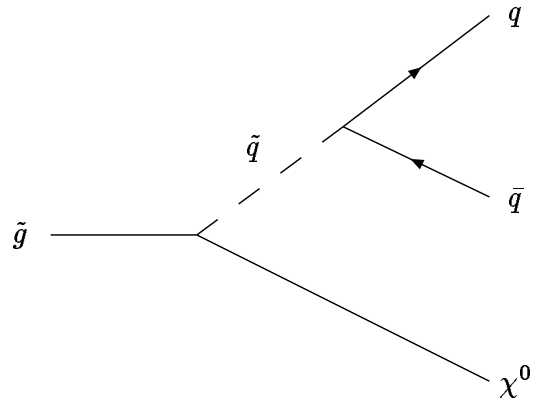


Figure 1: The dominant decay mode for gluinos, if they are lighter than the squarks, where  $\chi^0$  is a neutralino.

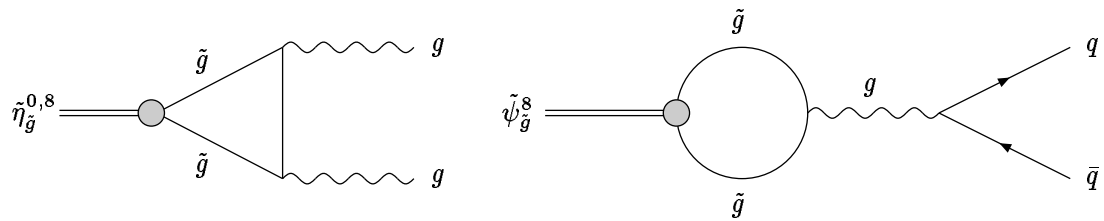


Figure 2: The dominant decay mechanisms for (a) pseudoscalar and (b) vector gluonium. The dominant production processes in hadron collisions are obtained by reading the diagrams from the right.

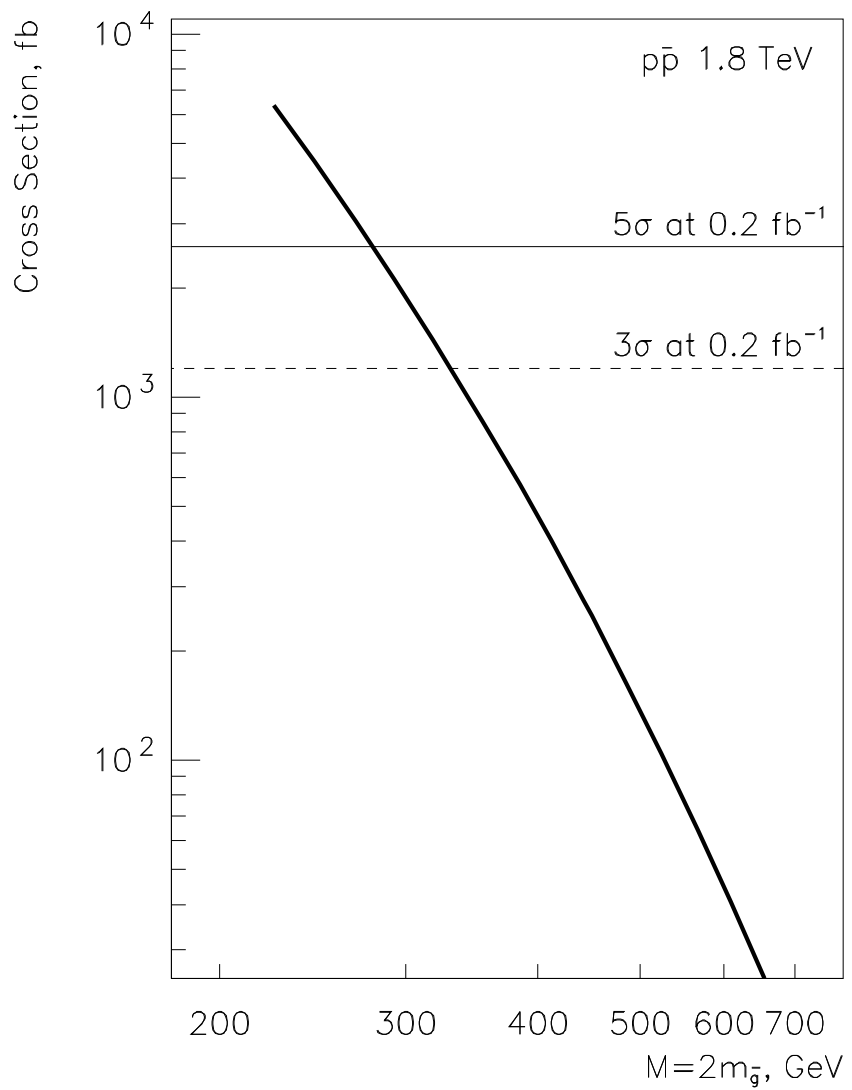


Figure 3: The calculated production cross section of vector gluonium in  $p\bar{p}$  collisions at 1.8 TeV. The solid and broken horizontal lines indicate the cross sections corresponding to a statistical significance at the peak of 5 and 3 standard deviations respectively, for a luminosity of  $200 \text{ pb}^{-1}$ . (See the text for the cuts and resolutions used).

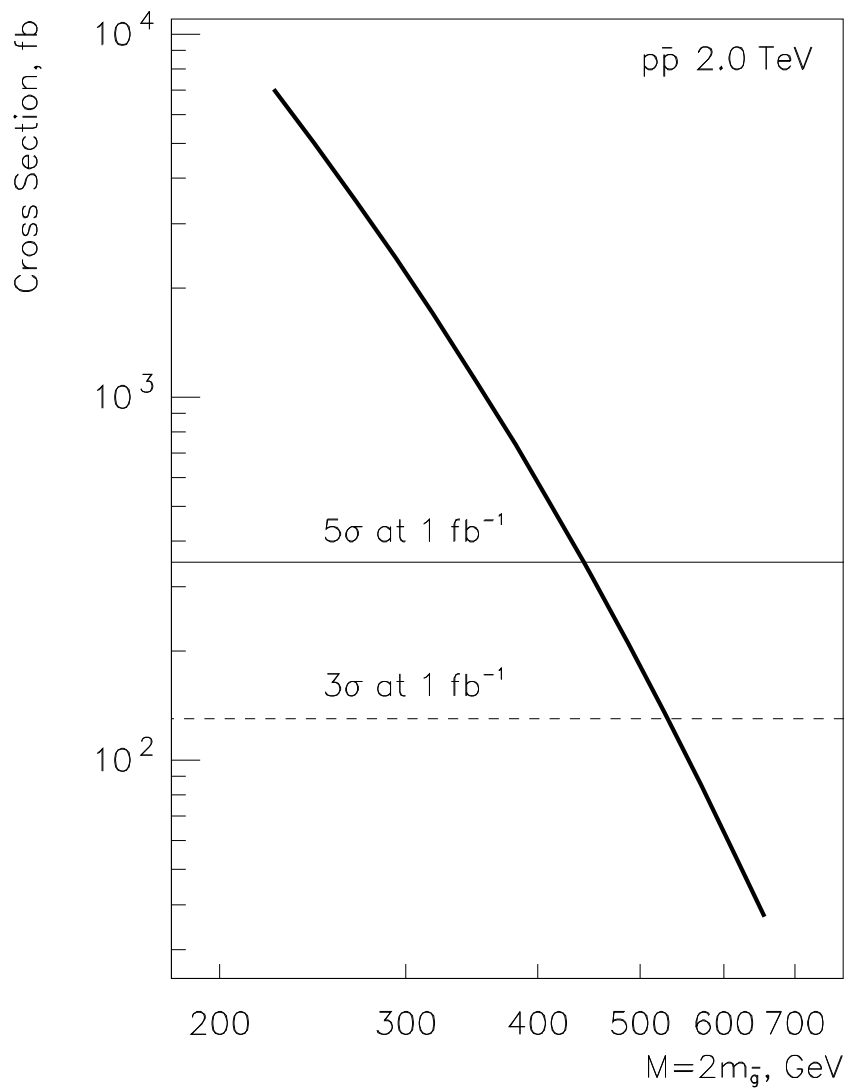


Figure 4: The calculated production cross section of vector gluonium in  $p\bar{p}$  collisions at 2.0 TeV. The solid and broken horizontal lines indicate the cross sections corresponding to a statistical significance at the peak of 5 and 3 standard deviations respectively, for a luminosity of  $1 \text{ fb}^{-1}$ . (See the text for the cuts and resolutions used).

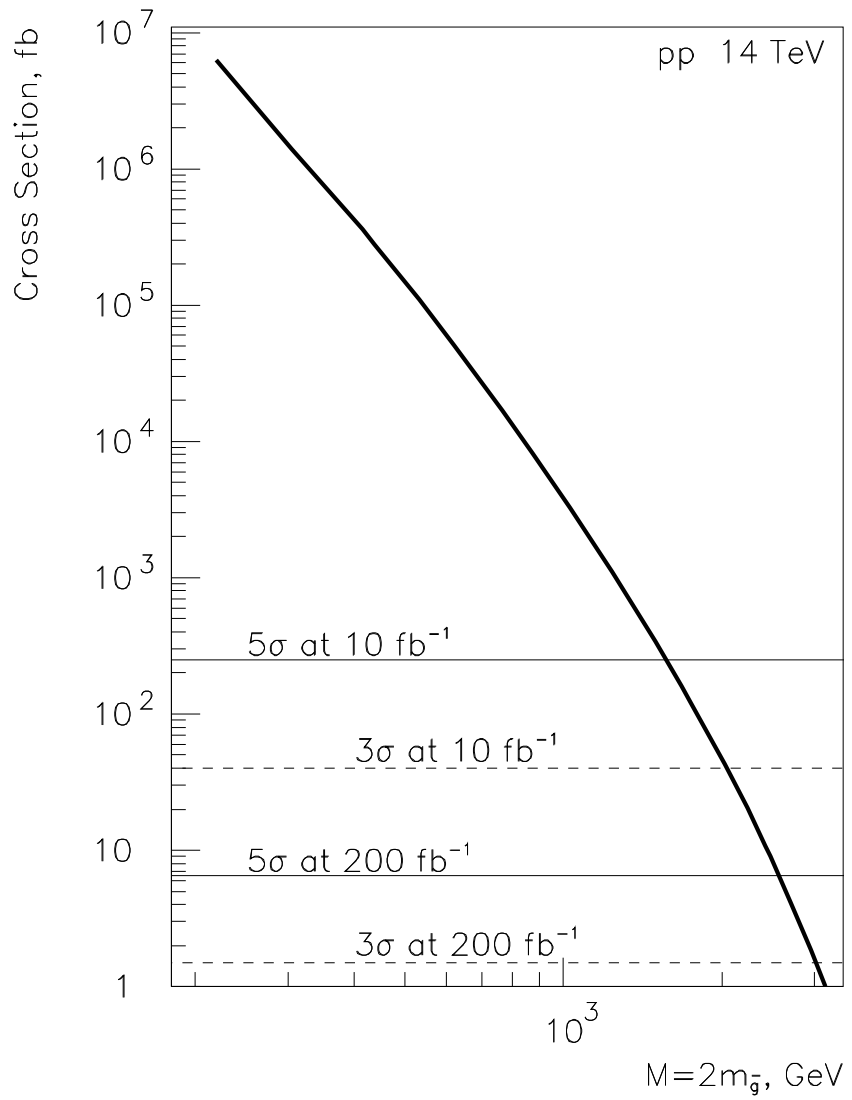


Figure 5: The calculated production cross section of pseudoscalar gluonium in  $pp$  interactions at 14 TeV. The solid and broken horizontal lines indicate the cross sections corresponding to a statistical significance at the peak of 5 and 3 standard deviations respectively, for two values of the luminosity:  $10^4 \text{ pb}^{-1}$  and  $2 \cdot 10^4 \text{ pb}^{-1}$ . (See the text for the cuts and resolutions used).